

DEVELOPMENT AND TESTING OF A SYSTEM FOR TIME-RESOLVED MEASUREMENT OF DROPLET SPECTRA IN STEAM TURBINES

M. Schatz*
 Institute of Thermal Turbomachinery
 and Machinery Laboratory
 University of Stuttgart
 70569 Stuttgart
 Germany

T. Eberle
 Roche Diagnostics GmbH
 68305 Mannheim
 Germany

D. M. Vogt
 Institute of Thermal Turbomachinery
 and Machinery Laboratory
 University of Stuttgart
 70569 Stuttgart
 Germany

ABSTRACT

Condensation in steam turbines is an inherently unsteady process because of the wake chopping from upstream blade rows. The increased dissipation in the wakes leads to considerable temperature fluctuations within the flow. For multistage turbines these fluctuations have been estimated to be in the range of 10% - 30% of the average stage enthalpy drop [1]. This also affects steam subcooling and the location of the onset of nucleation. As a consequence, the droplet spectrum found within steam turbines is not monodisperse but rather wide or even polymodal with larger droplets present.

The presence of unsteady condensation has quite a number of implications for the wetness losses in steam turbines, as the major contributors, e.g. thermodynamic losses and droplet drag, are directly affected. The same applies for droplet deposition and hence turbine blade erosion threat.

Up to now, a time-resolved measurement of the droplet spectra in steam turbines has not been performed, mainly because there is a lack of spectrometers operating at sufficiently high sampling rates. In this paper, the development of a system for time-resolved measurements of droplet size and number in steam turbines is presented together with the results of first tests in an industrial steam turbine.

NOMENCLATURE

Latin symbols

D_{32}	Sauter-diameter, μm
D	droplet or particle diameter, μm

g	extinction, $1/\text{m}$
I	intensity, W/m^2
I_0	undisturbed intensity, W/m^2
N	number concentration, $1/\text{m}^3$
N_{ref}	reference number concentration
t	time, sec
t_{pitch}	blade passage passing time, sec

Greek symbols

λ	wavelength, nm
σ	standard deviation

Abbreviations

APD	Avalanche Photo Diode
BPF	Blade Passing Frequency

INTRODUCTION

To date, the phenomenon of condensation in steam turbines is still not fully understood. Despite the fact that a lot of effort has been put into the numerical modeling of condensation, the different processes occurring during nucleation and subsequent droplet growth as well as the behavior of the resulting two-phase flow cannot be predicted accurately enough to allow a proper assessment of wetness losses or erosion threat [2].

One of the reasons for this shortcoming is the dearth of suitable validation data. While some data is available for steady condensation in nozzles, there is absolutely insufficient data for unsteady condensation processes. Only few measurements of the unsteady pressure or Schlieren images for self-excited oscillations of condensation in nozzles are

*corresponding author, email: schatz@itsm.uni-stuttgart.de

available, e.g. in [3] or in [4], but no data on the transient behavior of the droplet spectra.

Generally, the onset and strength of condensation as well as the resulting droplet spectrum is a function of steam subcooling and local expansion velocity at nucleation onset. In steam turbines, the flow field is inherently unsteady due to wake chopping effects. The dissipation that comes along with this causes local fluctuations of temperature which affect the thermodynamic state of the steam and hence have a considerable impact on the condensation process [5]. The impact can range from a change in subcooling at the onset of nucleation at a fixed location, i.e. the throat of a blade passage, to a periodic movement of the nucleation front between blade rows. Apart from a variation of the losses associated with condensation, this may also result in oscillating aerodynamic shocks due to supercritical heat addition or increased droplet deposition and subsequent erosion.

As a consequence, a time-resolved measurement of droplet size and number is necessary, as this will allow to determine the impact of unsteady condensation on the resulting two phase flow and, on top of that, would provide suitable validation data for numerical simulations of condensing steam flows in turbines.

One way to measure the droplet spectra present in wet steam is the method of light extinction [6]. For this approach, the spectral attenuation of light due to scattering at droplets is used to calculate the droplet spectrum present. This method has already been widely used for measurements in steam turbines [2], [7], [8], [9], [10], however, up to now only for steady measurements, as the integration time of spectrometers available is usually orders of magnitudes higher than the allowable time increments required to resolve the passage of a blade pitch sufficiently.

A system for the measurement of light extinction at high frequencies to allow the time-resolved measurement of the droplet spectrum in steam turbines has been developed at the Institute of Thermal Turbomachinery and Machinery Laboratory (ITSM) at the University of Stuttgart. The detector unit is composed of three high-speed photodiodes, while a laser system with three different wavelengths is used as emitter.

OVERVIEW OF UNSTEADY CONDENSATION PHENOMENA

When steam is expanded below the saturation line in steam turbines or in nozzles, the onset of condensation is delayed. This is due to the fact that an energy barrier exists for the formation of nuclei on which condensation can take place. The steam becomes subcooled, i.e. its temperature is lower than the saturation temperature at the prevailing static pressure. As subcooling increases, the rate of

formation of nuclei increases exponentially until a sufficient number of the latter is present and condensation sets in. Both droplet number and droplet size are determined by the level of subcooling. The phase change then happens almost instantaneously together with the release of latent heat, which is transferred from the newly formed droplets to the surrounding steam, thus terminating the subcooling.

Depending on the level of subcooling reached, the release of latent heat can exceed a critical value in transonic and supersonic flows and cause an aerodynamic shock which interacts with the condensation process. For low supersonic speeds in the range between $Ma = 1 - 1.3$, there is no stable state of flow and a self-induced oscillation is established [11]. There are only a few documented measurements of the oscillating pressure and especially the fluctuating droplet spectrum that is formed in this process, for example those of Skillings [4], see Fig. 1

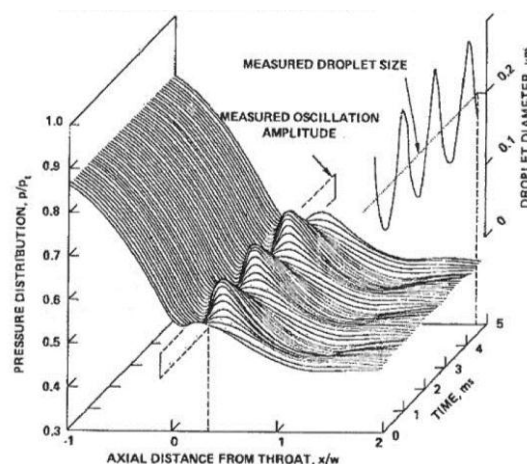


Fig. 1: Oscillating pressure and droplet size measured by Skillings [4]

In steam turbines the inherent unsteadiness of the flow caused by wakes of upstream blade rows also impacts on the condensation process. The dissipation within the wakes causes a local increase of temperature and hence enthalpy. In a theoretical study, Gyarmathy and Spengler [1] have estimated the enthalpy fluctuations of the flow in multistage turbines. They concluded that the amplitude of such fluctuations can amount to 30% of the overall stage enthalpy drop. It has to be mentioned, though, that these fluctuations have never been measured directly. Based on the work of Gyarmathy and Spengler, Guha and Young [5] have simulated the steam flow in a three stage and a six stage low pressure turbine using a throughflow code with pre-defined pitchwise loss coefficients coupled with a Lagrangian approach for the calculation of the thermodynamic state of steam. They found that the enthalpy fluctuations due to dissipation in wakes has a significant impact on the location of

condensation onset along a streamline, spreading the condensation onset across one or even two stages. Moreover, the steam subcooling level at condensation onset varies accordingly, hence giving a fluctuating droplet spectrum.

As common wetness measurement systems based on the light extinction method usually acquire data at integration times considerably longer than a blade passing period, these fluctuations cannot be measured, instead a broad polydispersed or even polymodal droplet spectrum is measured as the signal is averaged over several blade passing events.

As a consequence, it is not clear to date how large the fluctuations of droplet size and number in steam turbines really are and if for example steady state CFD-simulations can give a realistic picture of the processes happening in condensing steam flows in low pressure turbines. Especially for future applications, when it is envisaged to account for the effects of condensation already within the design process, for example for the assessment of erosion threat or for an estimate of wetness losses, a possibly transient nature of the condensation process must be taken into account.

SYSTEM DESCRIPTION

In order to determine a droplet spectrum based on the light extinction method, the extinction has to be measured at a number of discrete wavelengths. A summary of the light extinction method can be found in literature, e.g. in [6].

Measurement systems used for extinction measurements usually use white light (e.g. from halogene, deuterium or tungsten light sources) and then either a monochromator with narrow spectral filters in combination with a photodiode receiver, or a spectrometer in which the incoming light is split into the spectral components using a prism or an optical grating before the spectral intensities are measured using a CCD- or a CMOS-sensor array. In the first case the photodiode receiver would principally allow a time-resolved measurement, but the required monochromator for the spectral resolution inhibits a simultaneous measurement of several wavelengths. On the other hand, the CCD- or CMOS-sensors used in spectrometers generally require integration times in the range of milliseconds or even longer, depending on the light source used. This is about 1–2 orders of magnitude higher than the blade passing period in large scale power plant steam turbines, not to mention that of model turbines or industrial steam turbines.

As a consequence none of the systems used to date can be used for time-resolved measurements of light extinction and thus for transient wetness measurements. Therefore it has been decided to develop a new system designed for this purpose.

The development of the system is described in full length in [12].

For the specification of the required temporal resolution it has been decided that the new system must be able to do about 200 measurements within a blade passing period of the ITSM model steam turbine in order to be able to smooth the data prior to the analysis without major loss of information. As the blade passing frequency of the latter is in the range of approximately 10 kHz, this results in a sampling frequency of 2 MHz and maximum integration time for the receiver of 0.5 μ s. This does not only necessitate an extremely sensitive receiver sensor, but also requires the light input to be as large as possible to obtain a satisfactory sensor signal. Only APD-photodiodes are both sufficiently fast and sensitive for this purpose at comparably low noise.

To obtain high input intensities and to reduce the effort necessary to split the incoming light into its spectral components, a 3-color laser device with a light output power between 300 and 500 mW is used as light source. The wavelengths used are 445 nm (blue), 532 nm (green) and 638 nm (red).

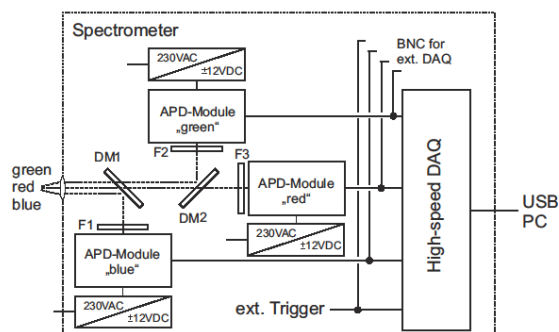


Fig. 2: Schematic drawing of the spectrometer design

To split the incoming light into its spectral components in the detector, a system of dichroic mirrors (DM) is used in the detector setup. Interference filters in front of the APDs are used to remove residual light of other wavelengths. A sketch of the detector setup is given in Fig. 2. The signal output of the APD-modules is recorded by a high-speed A/D-converter with a bandwidth of 20 MHz and a resolution of 12 bit. Figure 5 shows the response time of the APDs used. All three modules follow the step increase of intensity from a pulsed LED instantly with a rise time of less than 100 ns, i.e. about five times faster than required from the above stated specifications.

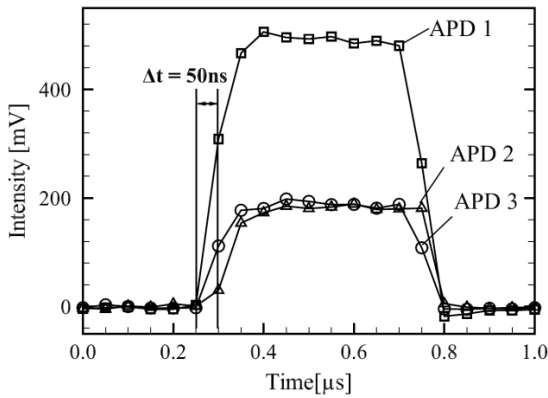


Fig. 3: Measured response times of all APDs used for the detector system

SYSTEM VALIDATION

In order to demonstrate the functionality of the new measurement system, static measurements with polystyrene particles of known size suspended in water were performed and analysed. The particle diameters used for this test were 107 nm and 2200 nm at standard deviations of ± 0.2 nm and ± 100 nm, respectively.

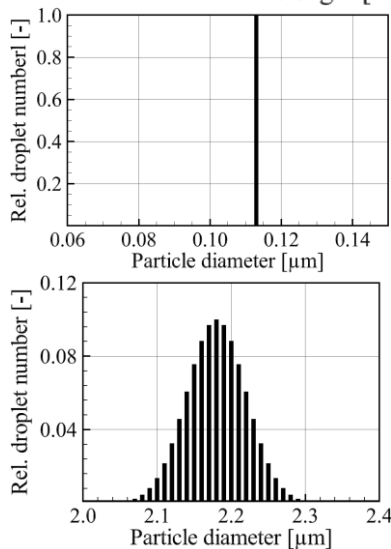
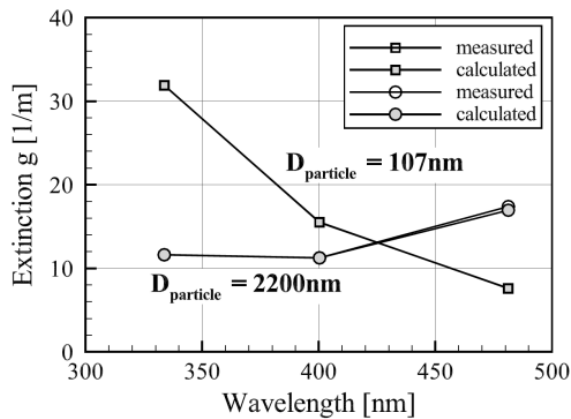


Fig. 4: Measured extinction and calculated size of polystyrene particles.

The measured extinctions together with the theoretical extinctions are shown in Fig. 4 (top). It

is quite evident from the figure that for both particle sizes the experimental data matches the theoretical perfectly.

The data analysis is based on the in-house code already used to analyse static measurements. It features both an inversion based on a non-negative least squares approach and a method based on various pre-defined mathematical distributions. The bottom figures in Fig. 4 show the results of the data analysis for both particle measurements. The monodisperse character of the 107 nm particles is captured as well as the polydisperse distribution of the larger 2200 nm particles. As a consequence, it can be stated that the data acquisition and analysis performs very well and is suited for the purpose of time-resolved wetness and droplet measurements.

To assess if an oscillating droplet spectrum can be resolved properly in general, a theoretical study was performed based on results of a numerical study of condensing steam flow in the nozzle used by Barschdorff [3]. The time-resolved droplet size and number from the simulation results was used to compute the course of relative intensity of the three wavelengths used for one oscillation period. This data was then processed and compared to the original input droplet spectrum. The calculated transient behavior of the droplet spectrum obtained from CFD together with the theoretical relative intensities is shown in Fig. 5. The results obtained with different approaches for the data analysis are plotted in Fig. 6. Both the behavior of the droplet size and droplet number compares very well with the input data. Only for the peak diameters of about 0.25 μm at $t \sim 1$ ms, the standard inversion method does overestimate the droplet size with 0.32 μm instead of 0.25 μm, consequently underestimating the droplet number. All other methods show a very good overall agreement with the original input data.

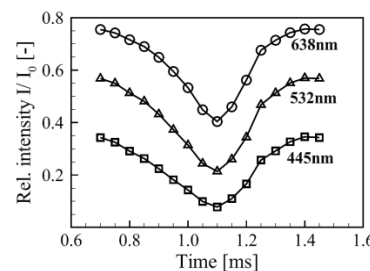
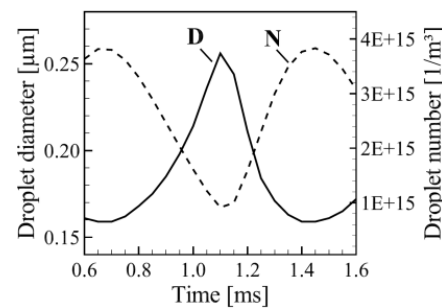


Fig. 5: Predicted droplet size and number fluctuation in a nozzle (top), resulting relative intensities (bottom)

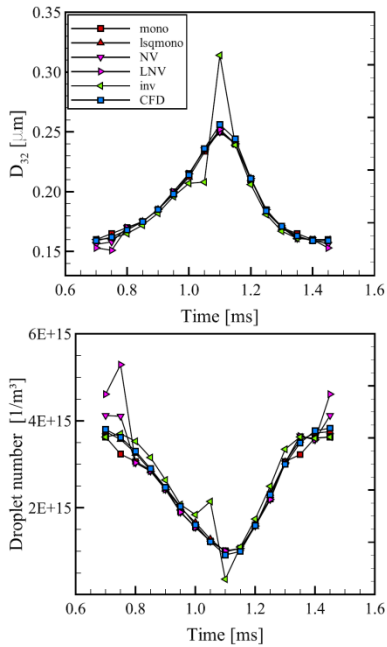


Fig. 6: Calculated droplet size and number after post-processing

ERROR ANALYSIS

The performance tests shown above were done for ideal signals, i.e. without any signal noise. Since the APD-modules exhibit a certain basic noise, this has to be taken into account with regard to the influence of noise on the inversion of extinction data to calculate the droplet spectrum. The standard deviations σ of the signal output of all three APDs were determined and added onto the theoretical intensities for three different intensity levels, namely 95%, 50% and 8% of the reference intensity at 445 nm. This was done for several different droplet diameters between 80 nm and 700 nm. The symbols in Fig. 7 show the calculated nominal intensities for an assumed droplet size of 80 nm, the variation due to detector noise is included as dotted lines for the raw signal (top figure) and for the case when a sliding average of 20 samples is used (bottom figure). The sliding average results in a considerable reduction of the noise for all three APDs. Due to the very high sampling frequency of 20 MHz, such an averaging does not result in a substantial loss of temporal resolution.

To assess the impact of noise on the result of the data analysis, based on the theoretical intensity spectra for each droplet size 100 noisy spectra were generated, whereby noise was added randomly in the range of $\pm 3\sigma$ of the corresponding APD. These intensity spectra were then processed to calculate the droplet diameters and the results were analysed statistically. To obtain a measure for the scatter of the results due to noise, the standard deviation of all calculated droplet diameters is normalized by the nominal diameter for which the intensity spectra have been calculated. Such a plot

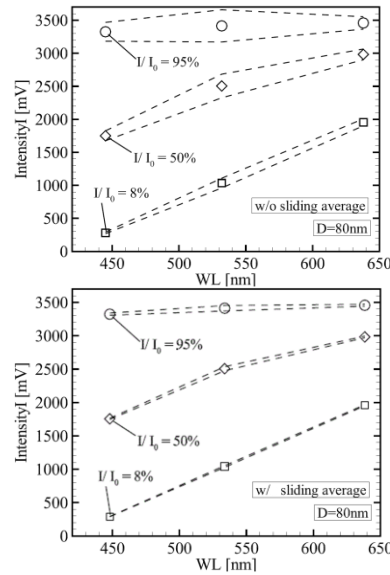


Fig. 7: Theoretical normalized intensities at different levels (symbols) and with additional noise (dotted lines)

is shown in Fig. 8 based on the noise measured with a moving average of 20 samples.

The most striking feature of Fig. 8 is that for low attenuation (95 % of the reference intensity at 445 nm) the sensitivity to noise is very high. For all investigated intensity levels, the possible error due to detector noise increases with decreasing droplet size, yet the influence of noise is negligible for higher attenuation and droplet diameters above approximately 150 nm.

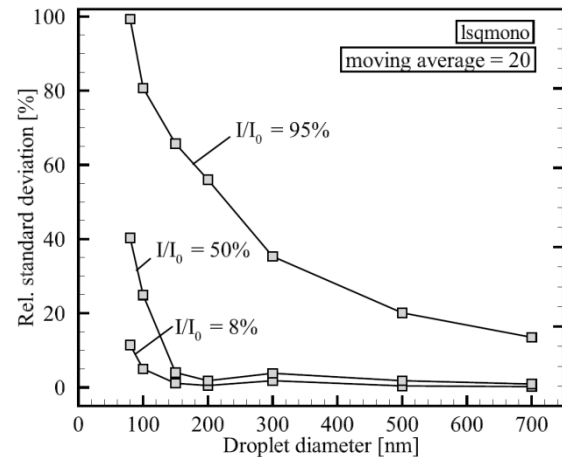


Fig. 8: Relative standard deviation of calculated droplet diameters with added noise

FIRST RESULTS

The new system was first tested in an industrial steam turbine. The wetness probe was installed downstream of the last stage in the upper part of the turbine. For transient measurements, the existing and proven combined optical/pneumatic probes which have been used for quite a number of steady measurements (e.g. [9], [10], [2]) can be used. Total and static pressure together with extinction can be measured simultaneously, thus

allowing to determine the flow vector as well as the thermodynamic state of the steam. Measurements were done at different span heights as indicated in Fig. 9.

Figure 10 shows a cutout of the measured extinction of the 445 nm wavelength that covers about three rotor revolutions at 80% span. It can be seen from the data that there are oscillations in the extinction signal – and hence in the droplet spectrum – which are at the same frequency as the rotor speed.

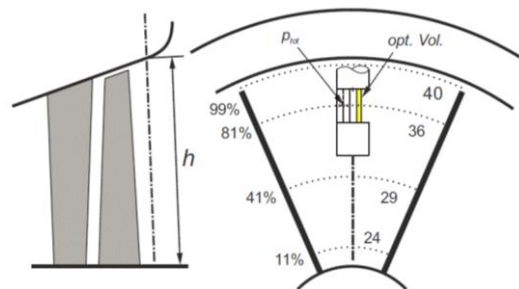


Fig. 9: Schematic drawing of the measurement locations behind the last stage

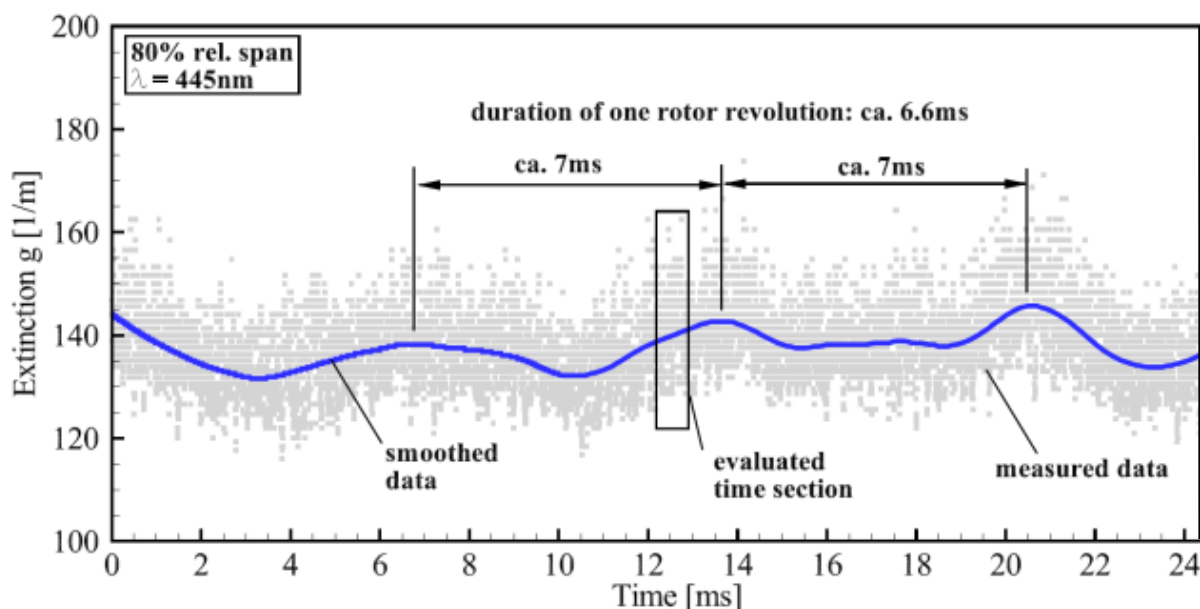


Fig. 10: Measured extinction for 445 nm at 80% span

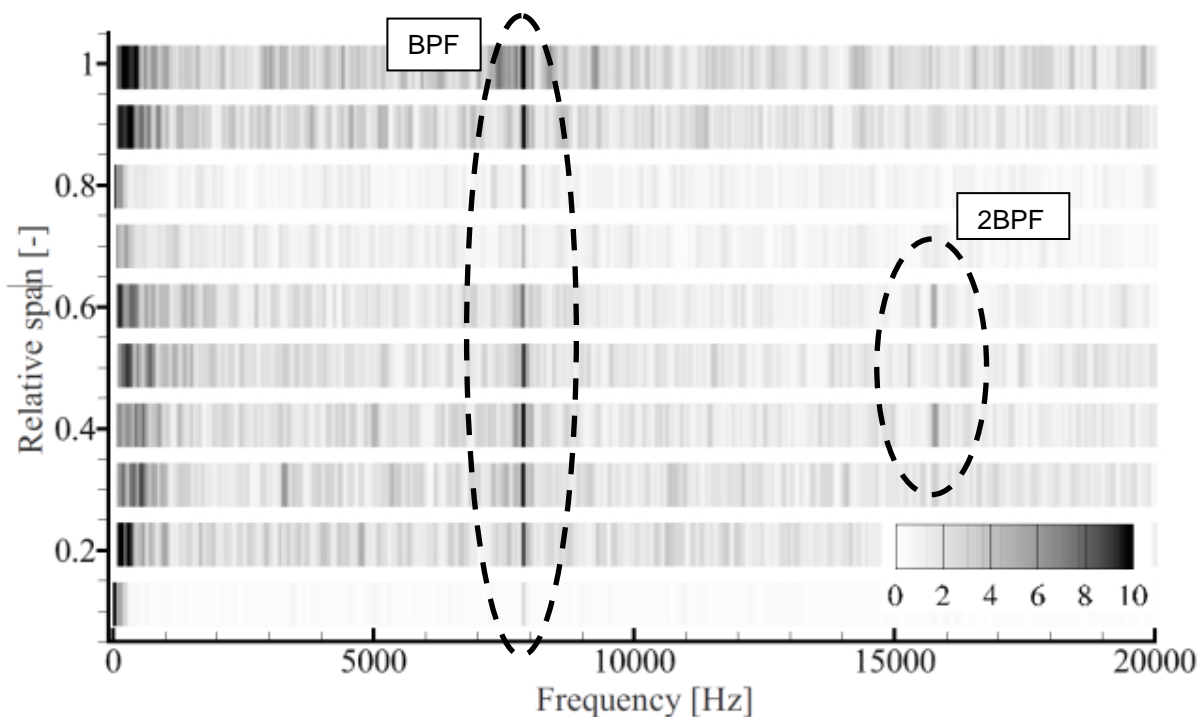


Fig. 11: Fourier spectrum of extinction signal along the span height

The amplitude spectrum of the extinction signal in the frequency domain is shown in Fig. 11 for all measured span heights. A 25 ms signal has been used for the Fourier Transformation, thus covering several rotor rotations. At all positions, the blade passing frequency (BPF) of approximately 8 kHz is dominant. At 40% and 60% span, the 2BPF-frequency is also visible. Moreover, there are relatively low amplitudes at 10% span as well as at 70% and 80% span. The latter span height is close to the location of the part span connector used to improve the mechanical robustness of the blades.

Three span heights will be discussed in more detail in the following section, namely 41% span, where both BPF and 2BPF are visible in the Fourier spectrum, 80% span, close to the location of the part span connector, and 99% span, covering the tip region of the blades and the tip leakage flow. The extinction signal for the wavelength of 445 nm at all three span heights can be seen in Fig. 12.

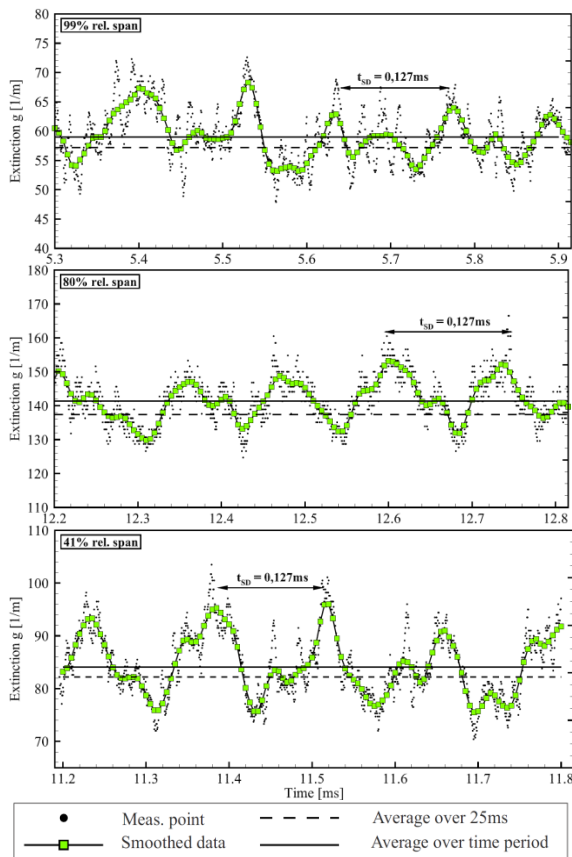


Fig. 12: Measured extinction at different span heights

The actually measured extinction is plotted in black dots, while the smoothed signal is denoted by the solid line and green rectangular symbols. Moreover, the average extinctions for a time window of 25 ms as used for Fig. 11 and for the duration of the cutout (0.6 ms) are indicated. The latter two averages are clearly different, thus underlining the conclusion drawn from Fig. 10 that

extinction and hence wetness also fluctuates at low frequency.

Clearly, the extinction and hence wetness varies considerably within a blade passage. The time difference between the signal peaks corresponds to the duration of a blade passage. Unfortunately, the course of the extinction signal can not be allocated to the position of the blade wakes, because no time-resolved pressure signal was measured. Interestingly, the amplitude fluctuation is about the same for all span heights with $\Delta g = \pm 10 \text{ m}^{-1}$. At 99% span, extinction is lowest, indicating smaller and/or fewer droplets than at the other span heights. Near the part span connectors, extinction is highest.

Results of the analysis of the measured extinction are shown in Fig. 13. All plots feature the course of calculated Sauter diameter D_{32} in the top part of each diagram and the course of the relative droplet number concentration at the bottom. The number concentration has been normalized for reasons of confidentiality.

The Sauter diameter at the blade tip at 99% span is fluctuating between about $0.48 \mu\text{m}$ and $0.55 \mu\text{m}$, while the normalized droplet number concentration varies considerably between 0.18 and 0.30, i.e. almost by a factor of 2. Especially in the course of the number concentration, the passage-wise variation of wetness is visible and the blade passing time is recognizable. The large fluctuation both in diameter and number concentration is very probably due to the influence of the tip vortex near the casing. As indicated by the comparably low extinction (see Fig. 12) the droplet size is lowest at this span height. At 80% span, the fluctuations of both droplet size and number concentration are considerably smaller. The Sauter diameter is fairly stable at about $0.82 \mu\text{m}$ and the number concentration slightly oscillates around 0.15. Nevertheless, the blade passing time can be identified. The relatively constant wetness structure at this location is quite amazing as one would expect a larger impact of the part span connector wake. At 41% span the Sauter diameter exhibits a higher fluctuation again, yet the number concentration is considerably more stable than at the blade tip.

The average droplet size and number concentration measured along the span downstream of the last stage is shown in Fig. 14. Both parameters are relatively stable between about 20% and 70% span. Only towards the hub and the casing some changes are noticeable. The droplet size increases at 80% span, before dropping towards the casing, while the number concentration increases at the same time. Near the hub, an increase of both droplet size and number can be seen.

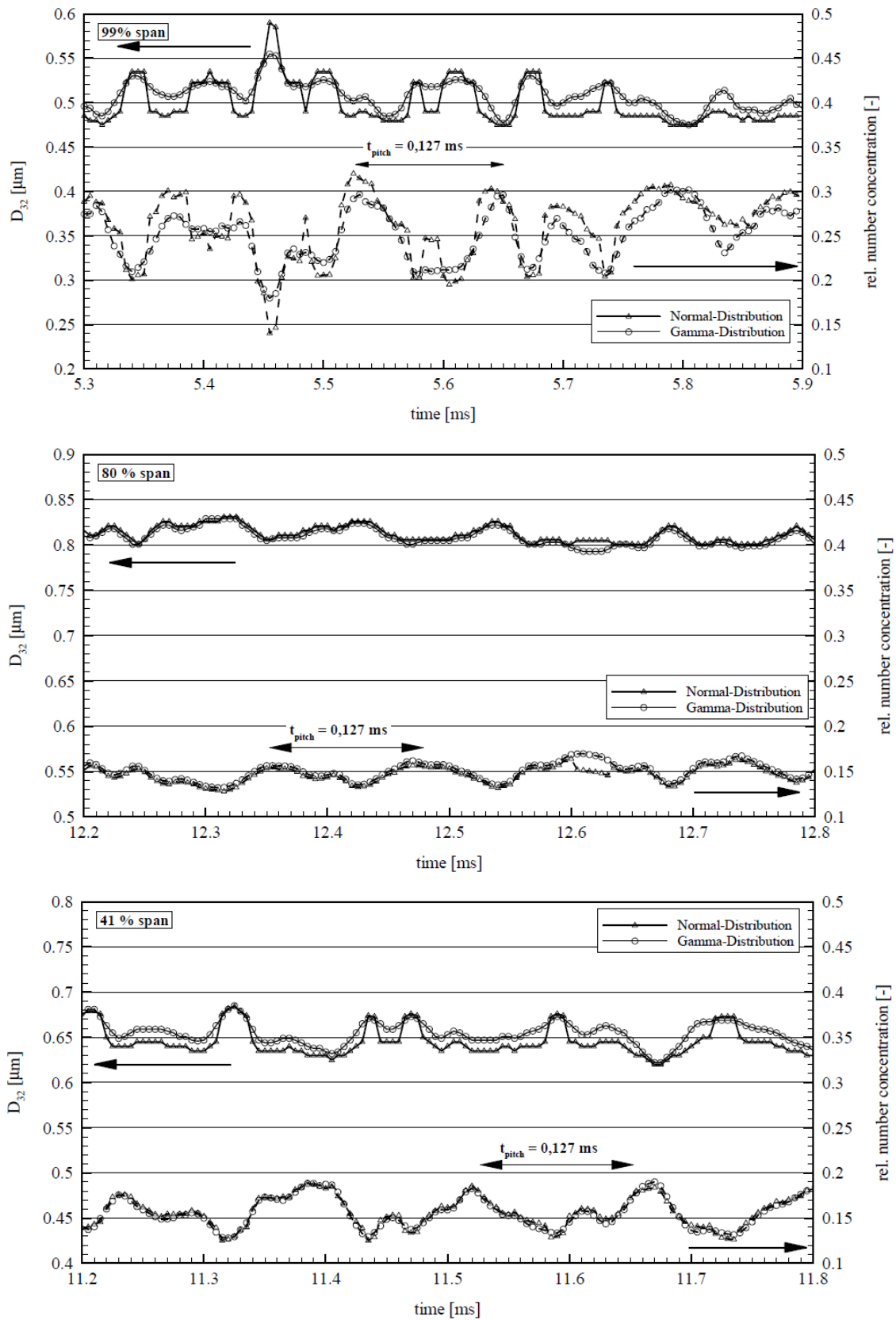


Fig. 13: Calculated droplet size and normalized number concentration at 99%, 80% and 41% span

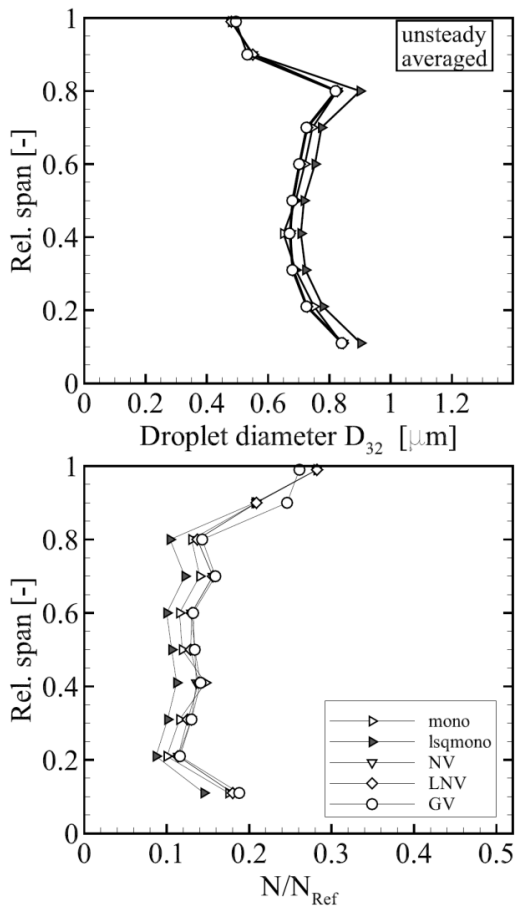


Fig. 14: Averaged droplet size and normalized number concentration along the span

CONCLUSIONS

The system for time-resolved measurement of droplet spectra in steam turbines that has been developed at ITSM has been validated and tested in an industrial steam turbine. The results show that the mean droplet diameter as well as the droplet number varies with blade passing frequency and partly with higher harmonics.

A comparison to steady measurements shows a good match between the results. Nevertheless, further tests have to be done to prove the applicability of the system. It is planned to use the system for measurements of self-excited condensation oscillations in nozzle flows as well as for further measurements in steam turbines. As a next step, transient total pressure sensors should be integrated into the probe in order to be able to allocate the observed fluctuations of droplet size and number to the flow structure, i.e. to be able to identify the wake of the passing blades. In addition, more measurements at different operating conditions are needed to get a more detailed picture of the impact of flow conditions on the wetness formed within the turbine, for example at part load conditions. On top of this, it would be very interesting to observe the behavior of the wetness structure during transient operation.

ACKNOWLEDGMENTS

The authors would like to express their gratitude to Dr. Thomas Polklas and Dr. Oliver Brunn from MAN Diesel & Turbo SE in Oberhausen, Germany.

REFERENCES

1. Gyarmathy G, Spengler P. Über die Strömungsfluktuationen in mehrstufigen thermischen Turbomaschinen. Traupel-Festschrift, Juris-Verlag Zürich. 1974:95–141. In German language.
2. Schatz M, Eberle T, Gruebel M, Starzmann J, Vogt DM, Suerken N. Two-Phase Flow Modeling and Measurements in Low-Pressure Turbines—Part II: Turbine Wetness Measurement and Comparison to Computational Fluid Dynamics-Predictions. *J. Eng. Gas Turbines Power*. 2015;137:42603.
3. Barschdorff D. Verlauf der Zustandsgrößen und gasdynamische Zusammenhänge bei der spontanen Kondensation reinen Wasserdampfes in Lavaldüsen. *Forsch Ing-Wes*. 1971;37:146–57. In German language.
4. Skillings SA, Moore MJ, Walters PT, Jackson R, Central Electricity Generating Board Leatherhead. A reconsideration of wetness loss in low pressure steam turbines: Central Electricity Generating Board (CEGB); 1988.
5. Guha A, Young J. The Effect of Flow Unsteadiness on the Homogeneous Nucleation of Water Droplets in Steam Turbines. *Philosophical Transactions of the Royal Society A: Mathematical, Physical and Engineering Sciences*. 1994;349:445–72.
6. Schatz M. Bestimmung der Zusammensetzung der Zweiphasen-Strömung in Niederdruck-Dampfturbinen auf der Grundlage der Lichtextinktionsmethode. Aachen: Shaker; 2012. In German language.
7. Walters PT. Wetness and Efficiency Measurements in L.P. Turbines With an Optical Probe As an Aid to Improving Performance. *J. Eng. Gas Turbines Power*. 1987;109:85.
8. Wroblewski W, Dykas S, Gardzilewicz K. M., 2009. Numerical and Experimental Investigation of Steam Condensation in LP Part of a Large Power Turbine. *Trans. ASME, J. Fluids Eng*; 131.
9. Eberle T, Schatz M, Starzmann J, Gruebel M, Casey M. Experimental study of the effects of temperature variation on droplet size and wetness

fraction in a low-pressure model steam turbine. Proceedings of the Institution of Mechanical Engineers, Part A: Journal of Power and Energy. 2014;228:97–106.

10. Schatz M, Eberle T. Experimental study of steam wetness in a model steam turbine rig: presentation of results and comparison with computational fluid dynamics data. Proceedings of the Institution of Mechanical Engineers, Part A: Journal of Power and Energy. 2014;228:129–42.

11. Gyarmathy G. Grundlagen einer Theorie der Nassdampfturbine: Diss. Techn. Wiss. ETH Zürich, Nr. 3221, 1962. In German language

12. Eberle T. Entwicklung und Erprobung eines optischen Messsystems zur Untersuchung von instationären Nässephänomenen in Düsen und Dampfturbinen. Doctoral Thesis; to be published.